Available online at www.sciencedirect.com
SCIENCE DIRECT®
Bioorganic & Medicinal Chemistry Letters 16 (2006) 437–442
Bioorganic & Medicinal Chemistry Letters

Carbonic anhydrase inhibitors: Valdecoxib binds to a different active site region of the human isoform II as compared to the structurally related cyclooxygenase II 'selective' inhibitor celecoxib

Anna Di Fiore,[a] Carlo Pedone,[a,b] Katia D'Ambrosio,[a] Andrea Scozzafava,[c] Giuseppina De Simone[a,*] and Claudiu T. Supuran[c,*]

[a]*Istituto di Biostrutture e Bioimmagini-CNR, via Mezzocannone 16, 80134 Naples, Italy*
[b]*Dipartimento delle Scienze Biologiche-Sezione Biostrutture, University of Naples "Federico II," via Mezzocannone 16, 80134 Naples, Italy*
[c]*Università degli Studi di Firenze, Polo Scientifico, Laboratorio di Chimica Bioinorganica, Room 188, Via della Lastruccia 3, 50019 Sesto Fiorentino (Florence), Italy*

Received 29 July 2005; revised 12 September 2005; accepted 15 September 2005
Available online 14 November 2005

Abstract—The high resolution X-ray crystal structure of the adduct of human carbonic anhydrase (CA, EC 4.2.1.1) isoform II (hCA II) with the clinically used painkiller valdecoxib, acting as a potent CA II and cyclooxygenase-2 (COX-2) inhibitor, is reported. The ionized sulfonamide moiety of valdecoxib is coordinated to the catalytic Zn(II) ion with a tetrahedral geometry. The phenyl-isoxazole moiety of the inhibitor fills the active site channel and interacts with the side chains of Gln92, Val121, Leu198, Thr200, and Pro202. Its 3-phenyl group is located into a hydrophobic pocket, simultaneously establishing van der Waals interactions with the aliphatic side chain of various hydrophobic residues (Val135, Ile91, Val121, Leu198, and Leu141) and a strong offset face-to-face stacking interaction with the aromatic ring of Phe131 (the $\chi 1$ angle of which is rotated of about 90° with respect to what was observed in the structure of the native enzyme and those of other sulfonamide complexes). Celecoxib, a structurally related COX-2 inhibitor for which the X-ray crystal structure was reported earlier, binds in a completely different manner to hCA II as compared to valdecoxib. Celecoxib completely fills the entire CA II active site, with its trifluoromethyl group in the hydrophobic part of the active site and the *p*-tolyl moiety in the hydrophilic one, not establishing any interaction with Phe131. In contrast to celecoxib, valdecoxib was rotated about 90° around the chemical bond connecting the benzensulfonamide and the substituted isoxazole ring allowing for these multiple favorable interactions. These different binding modes allow for the further drug design of various CA inhibitors belonging to the benzenesulfonamide class.

A recently developed class of pharmacological agents incorporating primary sulfamoyl moieties in their molecule is constituted by the cyclooxygenase-2 (COX-2) selective inhibitors acting as painkillers, with at least two clinically used drugs, valdecoxib **1** and celecoxib **2**.[1–3] It has recently been shown by our group[2] that such sulfonamide COX-2 'selective' inhibitors (unlike the methylsulfone ones, such as rofecoxib—Vioxx™) also act as potent inhibitors of several isoforms of the metallo-enzyme carbonic anhydrase (CA, EC 4.2.1.1),[4–6] some of which are strongly involved in tumorigenesis.[7–9] Although the selectivity issue of this class of pharmacological agents has very much been challenged ultimately, leading to the withdrawal of Vioxx from the market by Merck,[3] the potent antitumor activities of celecoxib and valdecoxib may still be exploited clinically, being probably due also to the inhibition of the tumor-associated CA isoforms CA IX and CA XII.[2,3]

In a previous work from this laboratory,[10] we have investigated the interaction of coxibs **1** and **2**, as well as that of the clinically used, classical sulfonamide CA

Keywords: Carbonic anhydrase; Isoform II; X-ray crystallography; Sulfonamide; Valdecoxib; Celecoxib; Acetazolamide; COX-2 selective inhibitors.
* Corresponding authors. Tel.: +39 081 2534579; fax: +39 081 2536642 (G.D.S.); tel.: +39 055 4573005; fax: +39 055 4573385 (C.T.S.); e-mail addresses:gdesimon@unina.it

0960-894X/$ - see front matter © 2005 Elsevier Ltd. All rights reserved.
doi:10.1016/j.bmcl.2005.09.040

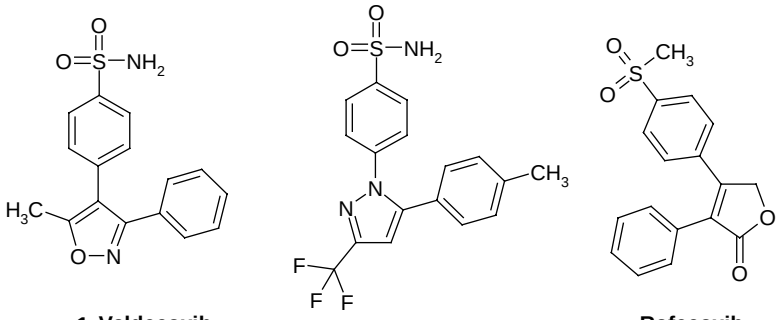

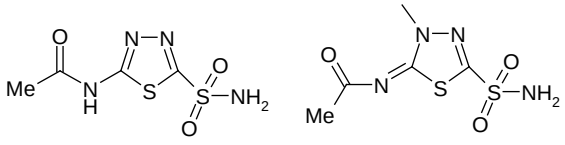

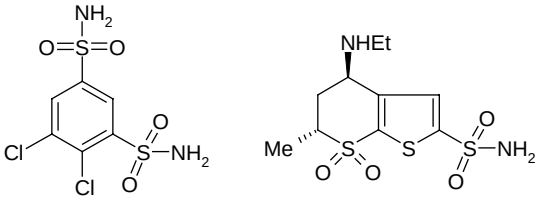

inhibitors acetazolamide **3**, methazolamide **4**, dichlorophenamide **5**, and dorzolamide **6** with several physiologically relevant CA isozymes, such as CA I and II (cytosolic forms), CA IV and CA IX (membrane-associated isozymes). Furthermore, the X-ray crystal structure of the hCA II—celecoxib adduct has been resolved at high resolution,[10] explaining thus at the molecular level why these COX-2 'selective' inhibitors also interact in a very favorable manner with the CA active site, leading to nanomolar COX-2/CA inhibitors (it may thus be clearly stated that these compounds are not at all selective inhibitors). In the same paper, we showed that similar to the classical sulfonamide CA inhibitors of types **3**–**6**, coxibs **1** and **2** are also useful as systemically/topically acting antiglaucoma agents in an animal model of the disease.[10]

To better understand the interactions of these agents with the CAs and also with the purpose of using such data for the rational drug design of benzenesulfonamide-based inhibitors, we report here a high resolution X-ray crystallographic study for the adduct of valdecoxib **1** with the physiologically most relevant and widespread CA isozyme, i.e., hCA II.[4–6] We also report here, for the first time, the inhibition data of coxibs **1** and **2** against the tumor-associated isoform hCA XII.[11]

Data of Table 1[12,13] clearly show that coxibs **1** and **2** act as weak inhibitors (K_Is in the range of 50–54 μM) of the cytosolic slow isozyme hCA I (similar to the clinically used topically acting sulfonamide dorzolamide **6**),[14] whereas the other investigated sulfonamides of types **3**–**5** are much more effective inhibitors of this isozyme (K_Is in the range of 50–1200 nM). Against the

Table 1. CA inhibition data with standard, clinically used sulfonamide inhibitors (**3**–**6**) and the COX-2 selective inhibitors valdecoxib **1** and celecoxib **2**

Compound	Inhibitor	K_I (nM)[a]				
		hCA I[b]	hCA II[b]	bCA IV[c]	hCA IX[d]	hCA XII[d]
1	Valdecoxib	54,000	43	340	27	13
2	Celecoxib	50,000	21	290	16	18
3	Acetazolamide	250	12	70	25	5.7
4	Methazolamide	50	14	36	27	3.4
5	Dichlorophenamide	1200	38	380	50	50
6	Dorzolamide	50,000	9	43	52	3.5

[a] Errors in the range of 5–10% of the reported values, from three determinations.
[b] Human cloned isozymes, esterase assay method.[12]
[c] Isolated from bovine lung microsomes, esterase assay method.
[d] Human cloned isozymes (catalytic domain), CO_2 hydrase assay method.[13]

physiologically most relevant isoform, hCA II, the two coxibs **1** and **2** show good inhibitory activity, with inhibition constants in the range of 21–43 nM, of the same order of magnitude as the clinically used sulfonamides **3**–**6** (K_Is in the range of 9–38 nM). The membrane-bound isoform of bovine origin bCA IV also showed lower affinity for coxibs **1** and **2** (K_Is in the range of 290–340 nM, in the same range as that of dichlorophenamide **5**), whereas the other sulfonamides behaved as better inhibitors of this isozyme (K_Is in the range of 36–70 nM for compounds **3**, **4**, and **6**). Similar to hCA II, the two tumor-associated isozymes hCA IX and hCA XII were prone to inhibition by coxibs **1** and **2**, which showed inhibition constants in the range of 16–27 nM against hCA IX, and 13–18 nM against hCA XII, respectively. These values are in the same range as those of the other sulfonamides investigated here, of types **3**–**6** (Table 1), and may explain the significant antitumor activity[7–9] of such compounds.

To understand the molecular basis responsible for the high binding affinity of valdecoxib **1** toward hCA II, and also the differences of inhibition between **1** and **2**, we solved the crystal structure of valdecoxib **1** complexed to hCA II.[15] The three-dimensional structure was analyzed by different Fourier techniques, the crystals being isomorphous to those of the native enzyme.[19] The model was refined using the CNS program[17] to crystallographic *R*-factor and *R*-free values of 0.185 and 0.200, respectively. The statistics for data collection and refinement are shown in Table 2. The overall quality of the model was high, with 100% of the non-glycine residues located in the allowed regions of the Ramachandran plot.

Table 2. Crystal parameters, data-collection, and refinement statistics for the hCA II–valdecoxib **1** adduct

Crystal parameters	
Space group	$P2_1$
Unit-cell parameters (Å, °)	$a = 42.05$
	$b = 41.32$
	$c = 71.76$
	$\beta = 104.26$
Data-collection statistics (20.00–1.46 Å)	
Temperature (K)	100
Total reflections	134,163
Unique reflections	39914
Completeness (%)	96.0 (91.7)
R_{sym}[a]	0.073 (0.244)
Mean *I*/sigma (*I*)	15.0 (4.9)
Refinement statistics (20.00–1.46 Å)	
R-factor[b](%)	18.5
R-free[b] (%)	20.0
rmsd from ideal geometry:	
Bond lengths (Å)	0.005
Bond angles (°)	1.4
Number of protein atoms	2084
Number of inhibitor atoms	22
Number of water molecules	342
Average *B* factor (Å^2)	13.71

Values in parentheses refer to the highest resolution shell.
[a] $R_{sym} = \Sigma|I_i - \langle I\rangle|/\Sigma I_i$; over all reflections.
[b] *R*-factor = $\Sigma||F_o| - |F_c||/\Sigma|F_o|$; *R*-free calculated with 5% of data withheld from refinement.

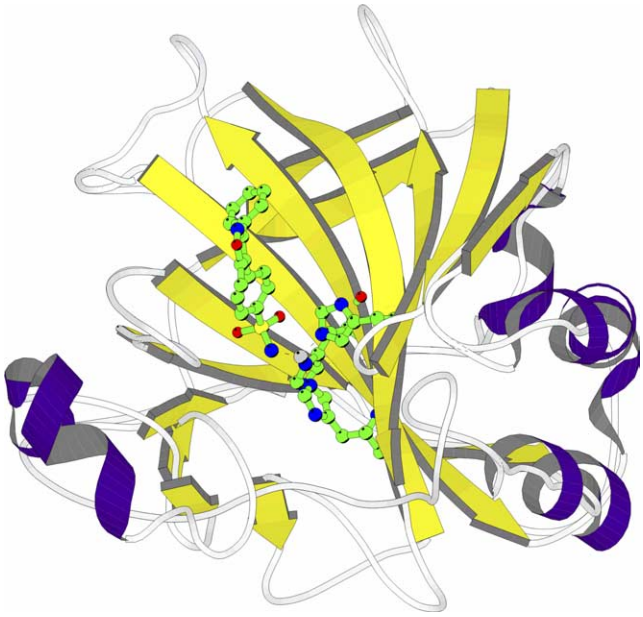

Figure 1. Ribbon diagram of the hCA II–valdecoxib **1** complex. The inhibitor, metal coordinating residues His94, His96, His119 and the zinc ion are represented in ball and stick.

In particular, the analysis of the electron density maps around the catalytic site allowed us to locate one inhibitor molecule into the active cavity of the enzyme. The topology of the inhibitor binding to the hCA II active site is shown in Figure 1. The structure of the enzyme in the valdecoxib–hCA II complex exhibited only minor conformational changes when compared to that of the native protein, with a rmsd of 0.35 Å. Clear electron density was visible for the entire inhibitor (Fig. 2) and the protein, except for the first two N-terminal residues.

Several polar and hydrophobic interactions stabilized the inhibitor within the hCA II active site. Indeed, the ionized N atom of the sulfonamide moiety of valdecoxib is coordinated to the catalytic Zn(II) ion with a tetrahedral geometry (N1–Zn(II) = 1.91 Å), displacing the hydroxide ion usually present in the active site of the uninhibited enzyme.[19] In addition, this nitrogen atom was also hydrogen bonded to the hydroxyl group of Thr199 (N1–ThrOG = 2.73 Å), which in turn interacted with the Glu106OE1 atom (2.55 Å). On the other hand, one sulfonamide oxygen was hydrogen bonded to the backbone amide of Thr199 (ThrN–O1 = 2.80 Å), whereas the other one was at a distance of 2.96 Å from the Zn(II) ion. All these interactions have already been described for other sulfonamide/sulfamate-containing CA inhibitors for which the structure has been solved in complexes with various CA isozymes.[10,20–30]

The phenyl-isoxazole moiety of valdecoxib filled the active site channel of the enzyme and interacted with the side chains of Gln92, Val121, Leu198, Thr200, and

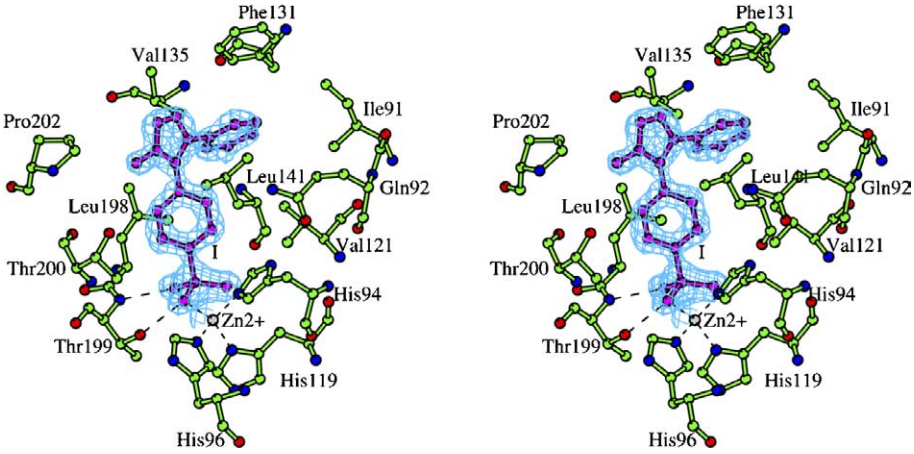

Figure 2. Stereo view of the active site region in the hCA II–valdecoxib complex. The simulated annealing omit $|2F_o - F_c|$ electron density map,[17] relative to the inhibitor molecule, is shown. Residues coordinating the metal ion and participating in recognition of the inhibitor molecule are also reported.

Pro202 (distance < 4.5 Å) (Fig. 2). Besides these interactions, the 3-phenyl group present in the inhibitor molecule was located into a hydrophobic cavity, simultaneously establishing van der Waals interactions with the aliphatic side chain of various hydrophobic residues (Val135, Ile91, Val121, Leu198, and Leu141) and a strong offset face-to-face stacking interaction with the aromatic ring of Phe131. To optimize the binding to valdecoxib, the $\chi 1$ angle of this latter residue (Phe131) was rotated about 90° with respect to what was observed in the structure of the native enzyme and the other complexes solved so far, and in which this type of interaction has been reported.[10,19–30]

Figure 3 shows a structural overlay of valdecoxib **1** and celecoxib **2**[10] bound to hCA II, as determined by the superposition of hCA II active site residues. It should be stressed again that both compounds are clinically used painkillers, mainly acting as COX-2 inhibitors (in addition to their strong CA inhibitory properties). In both cases, the organic scaffold of the inhibitor (i.e., the isoxazole ring of **1** or the pyrazole ring of **2**) did not establish polar interactions with the enzyme active site, but participated in a large number of hydrophobic contacts. This similarity was reflected by a rather comparable value of the K_I for the two inhibitors against hCA II (Table 1). However, even though valdecoxib and celecoxib are structurally similar, they show a very different location when bound to the enzyme active site. In fact, celecoxib completely filled the entire CA II active site, with its trifluoromethyl group in the hydrophobic part of the active site and the *p*-tolyl moiety in the hydrophilic one (and this may also explain why it is approximately a two times stronger hCA II inhibitor as compared to valdecoxib). Consequently, the *p*-tolyl moiety of celecoxib did not establish any interaction with the side chain of Phe131. In contrast to this, valdecoxib was rotated by about 90° around the chemical bond connecting the benzenesulfonamide and the substituted isoxazole ring. This rotation placed the 3-phenyl substituent of the inhibitor in a different position and allowed, together with the aforementioned movement of Phe131, the strong stacking interaction with this aromatic residue. It was, in fact, recently demonstrated by our group that just this interaction with Phe131 (or its absence) orients the active site binding region of inhibitors within the hCA II cavity,[30] allowing thus

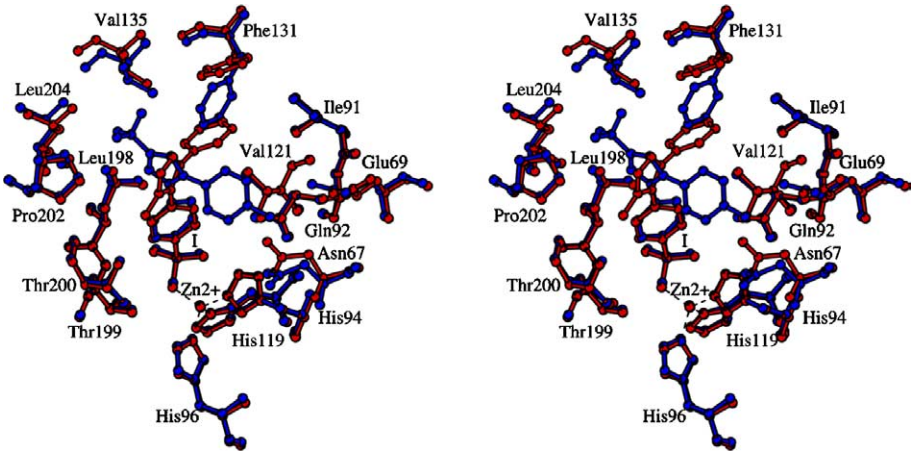

Figure 3. Stereo view of the hCA II active site complexed with valdecoxib **1** (red) and celecoxib **2**[10] (blue) brought to optimal structural overlay.

for further insights into the rational drug design of CA inhibitors.

In conclusion, the high resolution X-ray crystal structure of the adduct of hCA II with the clinically used painkiller valdecoxib, acting as a potent CA II and COX-2 inhibitor, is reported, showing that the sulfonamide moiety participates in the classical interactions with the Zn(II) ion, whereas the phenyl-isoxazole moiety interacts with residues Gln92, Val121, Leu198, Thr200, and Pro202. The 3-phenyl group of the inhibitor is located into a hydrophobic pocket and establishes van der Waals contacts with the aliphatic side chain of various hydrophobic residues and a strong offset face-to-face stacking interaction with the aromatic ring of Phe131. Celecoxib, a structurally related COX-2 inhibitor for which the X-ray crystal structure was reported earlier, binds in a completely different manner to hCA II as compared to valdecoxib. Celecoxib completely fills the entire CA II active site, with its trifluoromethyl group in the hydrophobic part of the active site and the *p*-tolyl moiety in the hydrophilic one, not establishing any interaction with Phe131. These different binding modes allow for the further drug design of various CA inhibitors belonging to the benzenesulfonamide class.

Acknowledgments

This research was financed in part by a grant from the 6th framework of EU (EUROXY project). We are very grateful to Professor Alexandru T. Balaban (Texas A&M University, USA) for helpful discussions that improved our manuscript. Thanks are also due to Sincrotrone Trieste CNR/Elettra for giving us the opportunity to collect data at the Crystallographic Beamline.

References and notes

1. de Leval, X.; Julémont, F.; Delarge, J.; Sanna, V.; Pirotte, B.; Dogné, J.-M. *Expert Opin. Ther. Pat.* **2002**, *12*, 969.
2. Supuran, C. T.; Casini, A.; Mastrolorenzo, A.; Scozzafava, A. *Mini-Rev. Med. Chem.* **2004**, *4*, 625.
3. Dogné, J.-M.; Supuran, C. T.; Pratico, D. *J. Med. Chem.* **2005**, *48*, 2251.
4. Supuran, C. T.; Scozzafava, A.; Casini, A. *Med. Res. Rev.* **2003**, *23*, 146.
5. Supuran, C. T.; Scozzafava, A. *Expert Opin. Ther. Pat.* **2002**, *12*, 217.
6. Scozzafava, A.; Mastrolorenzo, A.; Supuran, C. T. *Expert Opin. Ther. Pat.* **2004**, *14*, 667.
7. Pastorekova, S.; Parkkila, S.; Pastorek, J.; Supuran, C. T. *J. Enz. Inhib. Med. Chem.* **2004**, *19*, 199.
8. Švastová, E.; Hulíková, A.; Rafajová, M.; Zatovicová, M.; Gibadulinová, A.; Casini, A.; Cecchi, A.; Scozzafava, A.; Supuran, C. T.; Pastorek, J.; Pastoreková, S. *FEBS Lett.* **2004**, *577*, 439.
9. Cecchi, A.; Hulikova, A.; Pastorek, J.; Pastoreková, S.; Scozzafava, A.; Winum, J.-Y.; Montero, J.-L.; Supuran, C. T. *J. Med. Chem.* **2005**, *48*, 4834.
10. Weber, A.; Casini, A.; Heine, A.; Kuhn, D.; Supuran, C. T.; Scozzafava, A.; Klebe, G. *J. Med. Chem.* **2004**, *47*, 550.
11. Vullo, D.; Innocenti, A.; Nishimori, I.; Pastorek, J.; Scozzafava, A.; Pastorekova, S.; Supuran, C. T. *Biorg. Med. Chem. Lett.* **2005**, *15*, 963.
12. Pocker, Y.; Stone, J. T. *Biochemistry* **1967**, *6*, 668.
13. Khalifah, R. G. *J. Biol. Chem.* **1971**, *246*, 2561, An SX.18MV-R Applied Photophysics stopped-flow instrument has been used for assaying the CA- catalyzed CO_2 hydration activity. Phenol red (at a concentration of 0.2 mM) has been used as indicator, working at the absorbance maximum of 557 nm, with 10 mM Hepes (pH 7.5) as buffer, 0.1 M Na_2SO_4 (for maintaining constant ionic strength), following the CA-catalyzed CO_2 hydration reaction for a period of 10–100 s. The CO_2 concentrations ranged from 1.7 to 17 mM for the determination of the kinetic parameters and inhibition constants. For each inhibitor at least six traces of the initial 5–10% of the reaction have been used for determining the initial velocity. The uncatalyzed rates were determined in the same manner and subtracted from the total observed rates. Stock solutions of inhibitor (1 mM) were prepared in distilled-deionized water with 10–20% (v/v) DMSO (which is not inhibitory at these concentrations) and dilutions up to 0.1 nM were done thereafter with distilled-deionized water. Inhibitor and enzyme solutions were preincubated together for 15 min at room temperature prior to assay, in order to allow for the formation of the E–I complex. The inhibition constants were obtained by non-linear least-squares methods using PRISM 3, from Lineweaver–Burk plots, as reported earlier,[10,11] and represent the mean from at least three different determinations. Recombinant enzymes were used in the assays, which were obtained as reported earlier by our group.[11]
14. Supuran, C. T.; Scozzafava, A.; Conway, J., Eds.; *Carbonic Anhydrase—Its Inhibitors and Activators*; CRC Press: Boca Raton, FL, 2004; pp 1–363.
15. The hCA II–valdecoxib complex was obtained by adding a 3-molar excess of the inhibitor to a 10 mg/mL protein solution in 100 mM Tris–HCl, pH 8.5. Crystals of the complex were obtained at 4 °C using the hanging drop vapor diffusion method. Drops of 2 μl, prepared by mixing 1 μl of complex solution with an equal volume of precipitant solution (2.6 M $(NH_4)_2SO_4$, 0.3 M NaCl in 100 mM Tris–HCl (pH 8.4), and 5 mM 4-(hydroxymercury)-benzoate), were suspended over wells containing 1.0 ml of precipitant. In about two days, crystals of 0.46 mm × 0.11 mm × 0.10 mm were grown. A complete dataset was collected at 1.46 Å resolution from a single crystal, at 100 K, at the Synchrotron source Elettra in Trieste, Italy, using a Mar CCD detector. Prior to cryogenic freezing crystals were transferred to the precipitant solution with the addition of 15% (w/v) glycerol. Diffracted intensities were processed using the HKL crystallographic data reduction package (Denzo/Scalepack).[16] Crystal data and data-collection statistics are given in Table 2. The structure of the native hCA II (PDB code 1CA2) was used as a starting model for rigid body refinement in CNS.[17] Water molecules were removed from the starting model prior to structure factor and phase calculations. Crystallographic *R*-factor and *R*-free, calculated in the 20.00–1.46 Å resolution range, based on the starting model coordinates, were 0.389 and 0.390, respectively. Fourier maps calculated with $3F_o - 2F_c$ and $F_o - F_c$ coefficients showed prominent electron density features in the active site region. After an initial refinement, limited to the enzyme structure (*R*-factor = 0.227 and *R*-free = 0.247), a model for the inhibitor molecule was easily built up and introduced into the atomic coordinate set for further refinement. Many cycles of

manual rebuilding, using the program O[18] and positional and temperature refinement using the program CNS[17], were necessary to reduce the crystallographic *R*-factor and *R*-free values (in the 20.00–1.46 Å resolution range) to 0.185 and 0.200, respectively. The statistics for refinement are summarized in Table 2. Coordinates and structure factors have been deposited with the Protein Data Bank (Accession code 2AW1).

16. Otwinowski, Z.; Minor, W. *Methods Enzymol.* **1997**, *276*, 307.
17. Brünger, A. T.; Adams, P. D.; Clore, G. M.; De Lano, W. L.; Gros, P.; Grosse-Kunstleve, R. W.; Jiang, J. S.; Kuszewski, J.; Nilges, M.; Pannu, N. S.; Read, R. J.; Rice, L. M.; Simonson, T.; Warren, G. L. *Acta Crystallogr. Sect. D.* **1998**, *54*, 905.
18. Jones, T. A.; Zou, J. Y.; Cowan, S. W.; Kjeldgaard, M. *Acta Crystallogr. Sect. A* **1991**, *47*, 110.
19. Eriksson, A. E.; Jones, T. A.; Liljas, A. *Proteins Struct. Funct.* **1988**, *4*, 274.
20. Abbate, F.; Casini, A.; Owa, T.; Scozzafava, A.; Supuran, C. T. *Bioorg. Med. Chem. Lett.* **2004**, *14*, 217.
21. Abbate, F.; Casini, A.; Scozzafava, A.; Supuran, C. T. *Bioorg. Med. Chem. Lett.* **2004**, *14*, 2357.
22. Abbate, F.; Casini, A.; Scozzafava, A.; Supuran, C. T. *J. Enzyme Inhib. Med. Chem.* **2003**, *18*, 303.
23. Abbate, F.; Coetzee, A.; Casini, A.; Ciattini, S.; Scozzafava, A.; Supuran, C. T. *Bioorg. Med. Chem. Lett.* **2004**, *14*, 337.
24. Abbate, F.; Supuran, C. T.; Scozzafava, A.; Orioli, P.; Stubbs, M.; Klebe, G. *J. Med. Chem.* **2002**, *45*, 3583.
25. Abbate, F.; Winum, J.-Y.; Potter, B. V. L.; Casini, A.; Montero, J.-L.; Scozzafava, A.; Supuran, C. T. *Bioorg. Med. Chem. Lett.* **2004**, *14*, 231.
26. Casini, A.; Abbate, F.; Scozzafava, A.; Supuran, C. T. *Bioorg. Med. Chem. Lett.* **2003**, *13*, 2763.
27. Casini, A.; Antel, J.; Abbate, F.; Scozzafava, A.; David, S.; Waldeck, H.; Schä fer, S.; Supuran, C. T. *Bioorg. Med. Chem. Lett.* **2003**, *13*, 841.
28. Di Fiore, A.; De Simone, G.; Menchise, V.; Pedone, C.; Casini, A.; Scozzafava, A.; Supuran, C. T. *Bioorg. Med. Chem. Lett.* **2005**, *15*, 1937.
29. De Simone, G.; Di Fiore, A.; Menchise, V.; Pedone, C.; Antel, J.; Casini, A.; Scozzafava, A.; Wurl, M.; Supuran, C. T. *Bioorg. Med. Chem. Lett.* **2005**, *15*, 2315.
30. Menchise, V.; De Simone, G.; Alterio, V.; Di Fiore, A.; Pedone, C.; Scozzafava, A.; Supuran, C. T. *J. Med. Chem.* **2005**, *48*, 5721.